Frequency-Domain Analysis of N-path Filters Using Conversion Matrices

Sameed Hameed, *Student Member, IEEE,* Mansour Rachid, *Member, IEEE,* Babak Daneshrad, *Member, IEEE,* and Sudhakar Pamarti, *Member, IEEE*

***Abstract*—N-path filters are finding increased prominence in recent architectures for tunable transceivers. The clock-programmable center frequency together with programmable baseband bandwidth makes it a natural fit for wide programmability required in software-defined radios and cognitive radios. However, the analysis of such filters remain difficult due to their linear, periodically time-varying (LPTV) nature. This paper presents an analysis of N-path filters using conversion matrices. Conversion matrices allow analysis of an LPTV circuit with an equivalent frequency domain circuits that can in turn be analyzed similar to a linear time invariant (LTI) circuit. On applying this method to N-path filters, results already established in prior art are reproduced accurately. Further, effects of a few important non-idealities, such as clock overlaps, non-ideal clock duty cycles, and parasitic elements are also calculated and verified.**

***Index Terms*—Conversion matrices, LPTV circuit analysis, N-path filter, tunable filters, band-pass filters**

I. Introduction

WIDE programmability is increasingly important in transceiver designs. In fact, next generation architectures for wireless radios such as software-defined radios (SDRs) and cognitive radios (CRs) rely on such programmability [1], [2]. N-path filters [3] and the related mixer-first receivers are currently seen as excellent candidates for building such systems. Recent works [5], [6], [7], [11] have demonstrated the efficacy of such circuits towards this goal. Analysis of such circuits, which are from a class of circuits known as "linear, periodically time-varying" (LPTV) circuits, however, poses a formidable challenge. Generally, the periodically time-varying nature of such circuits (due to the presence of clock-driven switching elements) leads to frequency translation of the circuit's voltages and currents, and so traditional Laplace or Fourier domain linear time invariant (LTI) circuit analysis techniques have limited applicability.

Several techniques to analyze LPTV circuits have been reported. Since the circuit is linear, we can still use the impulse response to characterize it. However, due to the time-varying nature of the circuit, the impulse response is also time-varying, and hence depends on both the time t and the delay τ, and hence is represented by $h(t,\tau)$. Hence, the output, $y(t)$, is related to the input, $u(t)$, by the convolution:

$$y(t) = \int_{-\infty}^{\infty} u(t-\tau)h(t,\tau)d\tau. \tag{1}$$

Since the time-variation is periodic, the impulse response $h(t,\tau)$ is periodic in t by the fundamental period of the LPTV system, $T_p = 2\pi/\omega_p$. Hence, it can be expanded as a Fourier series as $h(t,\tau) = \sum_{n=-\infty}^{\infty} h_n(\tau)e^{jn\omega_p t}$. Substituting for $h(t,\tau)$ in (1), then taking the Fourier transform (in t) and simplifying gives:

$$\begin{aligned} Y(\omega) &= \sum_{n=-\infty}^{\infty} \widetilde{H}_n(\omega - n\omega_p)U(\omega - n\omega_p) \\ &= \sum_{n=-\infty}^{\infty} H_n(\omega)U(\omega - n\omega_p) \end{aligned} \tag{2}$$

where $U(\omega)$ and $Y(\omega)$ are the Fourier transforms of the input and output respectively, $\widetilde{H}_n(\omega)$ is the Fourier transform of $h_n(t)$, and the set of transfer functions, $H_n(\omega) = \widetilde{H}_n(\omega - n\omega_p)$, are known as the *"harmonic transfer functions"* (HTFs). Note that the HTFs are just recentered $\widetilde{H}_n(\omega)$ (by convention). Now, finding the HTFs becomes the goal of the circuit analysis [4]-[12]. Analogously in LTI systems only a single function, $H_0(\omega)$, which is the transfer function, is required. Several works derive the HTFs by applying circuit laws in the time domain and then applying a Fourier transform [6], [7]. State-space-based approaches, which treat the circuit as periodically moving through a set of states, have also been shown to be useful [8]-[11]. Ultimately, all such prior analysis techniques tend to be ad-hoc and a more systematic approach is desired.

This paper highlights an alternative method of analysis that uses the theory of conversion matrices. Conversion matrices have been extensively studied in literature in the area of computer simulation of complex time-varying circuits [13], and its use has even been extended to non-linear circuits [14], [15]. They have also been proven useful in studying noise in large RF circuits [16]. This paper provides a brief overview of conversion matrices. They are then applied to the analysis of a differential N-path filter to highlight their efficacy.

II. Conversion Matrices

To start, let us assume that $U(\omega)$ and $Y(\omega)$ in (2) are band-limited to $\omega\epsilon\left(-\left(K+\frac{1}{2}\right)\omega_p, \left(K+\frac{1}{2}\right)\omega_p\right]$, where $K \to \infty$ is a large positive integer. Then, let us define the frequency vector of a frequency transform of

This work was supported in part by the National Science Foundation under NSF grant ECCS 1408647.

S. Hameed, B. Daneshrad and S. Pamarti are with the Department of Electrical Engineering, University of California, Los Angeles, CA 90095 USA (e-mail: sameed@ucla.edu; babak@ee.ucla.edu; spamarti@ee.ucla.edu).

M. Rachid is with Silvus Technologies, Inc., 10990 Wilshire Blvd., Suite #1500, Los Angeles, CA 90024 USA (e-mail: mansour@silvustechnologies.com).

Table I
BASIC CONVERSION MATRICES

Component	LTI Relation	LPTV Relation	Illustration
Resistor	$V(\omega) = R\,I(\omega)$ $I(\omega) = R^{-1}V(\omega)$	$\underline{V}(\omega) = \mathbb{R}\underline{I}(\omega)$ $\underline{I}(\omega) = \mathbb{R}^{-1}\underline{V}(\omega)$	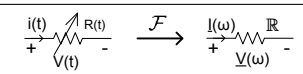
Capacitor	$I(\omega) = jC\omega V(\omega)$ $V(\omega) = -j\omega^{-1}C^{-1}I(\omega)$	$\underline{I}(\omega) = j\mathbb{C}\mathbf{\Omega}(\omega)\underline{V}(\omega)$ $\underline{V}(\omega) = -j\mathbf{\Omega}^{-1}(\omega)\mathbb{C}^{-1}\underline{I}(\omega)$	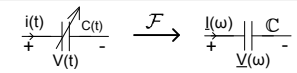
Inductor	$V(\omega) = jL\omega I(\omega)$ $I(\omega) = -j\omega^{-1}L^{-1}V(\omega)$	$\underline{V}(\omega) = j\mathbb{L}\mathbf{\Omega}(\omega)\underline{I}(\omega)$ $\underline{I}(\omega) = -j\mathbf{\Omega}^{-1}(\omega)\mathbb{L}^{-1}\underline{V}(\omega)$	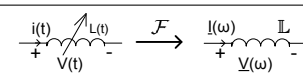
Controlled Source	$U_o(\omega) = \alpha U_i(\omega)$ $U_i(\omega) = \alpha^{-1}U_o(\omega)$	$\underline{U_o}(\omega) = \mathbb{A}U_i(\omega)$ $\underline{U_i}(\omega) = \mathbb{A}^{-1}\underline{U_o}(\omega)$	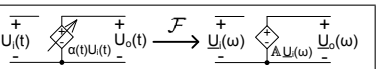
Series Combination	$V(\omega) = V_1(\omega) + V_2(\omega)$ $= (Z_1(\omega) + Z_2(\omega))\,I(\omega)$	$\underline{V}(\omega) = \underline{V_1}(\omega) + \underline{V_2}(\omega)$ $= (\mathbb{Z}_1(\omega) + \mathbb{Z}_2(\omega))\,\underline{I}(\omega)$	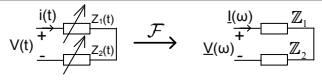
Parallel Combination	$I(\omega) = I_1(\omega) + I_2(\omega)$ $= (Y_1(\omega) + Y_2(\omega))\,I_1(\omega)$	$\underline{I}(\omega) = \underline{I_1}(\omega) + \underline{I_2}(\omega)$ $= (\mathbb{Y}_1(\omega) + \mathbb{Y}_2(\omega))\,\underline{V}(\omega)$	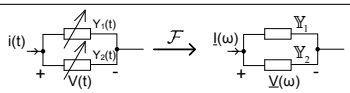

a signal $x(t)$ in an LPTV system as the vector $\underline{X}(\omega) = \left[\begin{array}{cccc} X(\omega - K\omega_p) & X(\omega-(K-1)\omega_p) & \cdots & X(\omega+K\omega_p) \end{array}\right]^T$, $\omega\epsilon\left(-\frac{1}{2}\omega_p, \frac{1}{2}\omega_p\right]$, where $X(\omega)$ is the Fourier transform of $x(t)$, and $T_p = 2\pi/\omega_p$ is the fundamental period of the system. Then defining frequency vectors, $\underline{U}(\omega)$ and $\underline{Y}(\omega)$ for the input and output of the system respectively, using (2), it can be shown that $\underline{Y}(\omega) = \mathbb{H}(\omega)\underline{U}(\omega)$, where the matrix

$$\mathbb{H}(\omega) = \begin{bmatrix} \vdots & \vdots & \vdots & \\ \cdots & H_{-1,-1}(\omega) & H_{-1,0}(\omega) & H_{-1,1}(\omega) & \cdots \\ \cdots & H_{0,-1}(\omega) & H_{0,0}(\omega) & H_{0,1}(\omega) & \cdots \\ \cdots & H_{1,-1}(\omega) & H_{1,0}(\omega) & H_{1,1}(\omega) & \cdots \\ & \vdots & \vdots & \vdots & \end{bmatrix} \quad (3)$$

is referred to as the conversion matrix (or the *"harmonic transfer matrix*" [12]) (of the LPTV system), and whose elements are given by $H_{i,j}(\omega) = H_{i-j}(\omega + i\omega_p)$, i.e. just frequency shifted HTFs.

By itself, (3) is just the matrix form of (2), and does not give any extra information. However, for simple switching components the HTFs, and hence $\mathbb{H}(\omega)$ can be easily derived [13]. For example, consider an LPTV capacitor, whose capacitance is varying as $C(t) = C(t + T_p)$. The voltage and the current across the capacitor are related in the time and frequency domains by the following relations:

$$i(t) = C(t)\frac{dV(t)}{dt} \overset{\mathcal{F}}{\longleftrightarrow} I(\omega) = C(\omega) * j\omega V(\omega)\,, \quad (4)$$

where $*$ is the convolution operator. Since $C(t)$ is periodic, it can be expanded as a Fourier series and its Fourier transform, $C(\omega)$, can be shown to be a sum of impulses at $\omega = m\omega_p$ with amplitudes C_m, where m is an integer, and C_m is the coefficient of $e^{jm\omega_p t}$ in the Fourier series expansion of $C(t)$: $C(\omega) = \sum_{m=-\infty}^{\infty} C_m\delta(\omega - m\omega_p)$. Then (4) gives:

$$I(\omega) = \sum_{m=-\infty}^{\infty} j(\omega - m\omega_p)\,V(\omega - m\omega_p)\,C_m. \quad (5)$$

Defining vectors $\underline{V}(\omega)$ and $\underline{I}(\omega)$ as before, (5) can be written in matrix form as $\underline{I}(\omega) = j\mathbb{C}\mathbf{\Omega}(\omega)\underline{V}(\omega)$, where $\mathbf{\Omega}(\omega) = diag\ \{[\omega - K\omega_p \quad \cdots \quad \omega \quad \cdots \quad \omega + K\omega_p]\}$, and

$$\mathbb{C} = \begin{bmatrix} C_0 & C_{-1} & \cdots & C_{-2K} \\ C_1 & C_0 & \cdots & C_{-2K+1} \\ \vdots & \vdots & \vdots & \vdots \\ C_{2K} & C_{2K-1} & \cdots & C_0 \end{bmatrix}. \quad (6)$$

The relation thus obtained, $\underline{I}(\omega) = j\mathbb{C}\mathbf{\Omega}(\omega)\underline{V}(\omega)$, is remarkably similar to the Fourier domain relation for a constant capacitor , i.e., $I(\omega) = jC\omega V(\omega)$. Hence $\mathbb{Y}_C(\omega) = j\mathbb{C}\mathbf{\Omega}(\omega)$ can be called the conversion matrix of the *"LPTV admittance"* of the switching capacitor. This relation is invertible for well-behaved capacitor variations, i.e. the conversion matrix of the *"LPTV impedance"* can be obtained by inverting the matrix of the LPTV admittance and vice versa. Similar relations can be obtained for all other LPTV elements, a subset of which is reported in Table I. Note that all matrices (such as $\mathbb{R}$, $\mathbb{L}$, $\mathbb{A}$, etc.) have the same form as $\mathbb{C}$ in (6).

The most important property of the frequency vectors is that they follow linearity. Hence, linear Kirchhoff's law relations that hold for time-domain voltage and current signals hold for their corresponding frequency vectors. This implies that other well known LTI results, such as series and parallel combination of impedances, Thevenin and Norton equivalent circuits, etc., have their conversion matrix equivalents as well. Hence by using such circuit laws, and basic conversion matrices (such as those in Table I), arbitrary LPTV circuits can be easily analyzed to derive their conversion matrices. To illustrate, this technique is applied to N-path filters.

III. N-PATH FILTERS

N-path filters were first proposed in [3]. The concept is simple: if a high-frequency RF input signal is first down-converted to around DC, passed through a low-pass filter, and then upconverted back to RF, then the input effectively sees a band-pass filter response. A simple implementation of this concept, the differential band-pass N-path filter is shown in Fig. 1(a) [11] (the differential filter is preferred over the single-ended version as it rejects DC and even harmonics of the switching frequency). The differential RF voltage input is connected though source resistors to a set of N parallel switched capacitor loads in succession, with the switches controlled by non-overlapping clocks with an ideal duty cycle of $\frac{1}{N}$, and a period, T_p, as shown in the figure. The number of paths, N, is even, and two paths are active at any one instant of time via the closing of two switches so that both ends of the differential input as connected to a load capacitor. The load capacitors, C, are chosen such that the bandwidth $2/NR_sC$ (the effective resistor seen by each capacitor is $NR_s/2$ due to the duty cycling) is much smaller than ω_p. The switches essentially downconvert and upconvert signals, while the resistor-capacitor combination behaves like a low-pass filter. The differential output voltage is then measured between the nodes $V_{o+}(t)$ and $V_{o-}(t)$ (the common nodes for the switches), and exhibits a band-pass response. This circuit can be easily analyzed using conversion matrices.

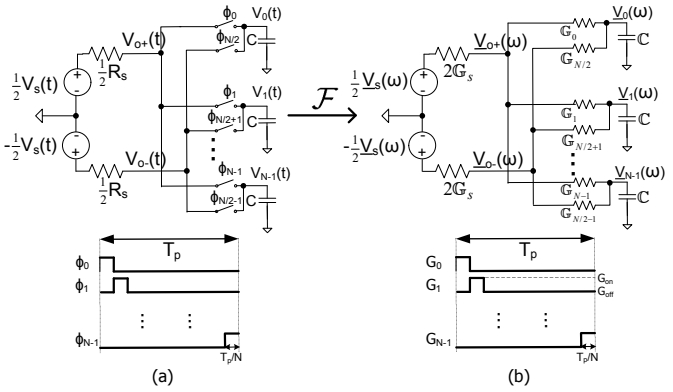

Figure 1. The differential band-pass N-path filter

Let $\mathbb{G}_i$ denote the conversion matrix of the LPTV conductance of the switch in the i^{th} branch, $\mathbb{G}_s = R_s^{-1}\mathbb{I}$ represent the source conductance, and $\mathbb{Y}_L = jC\mathbf{\Omega}(\omega)$ denote the LPTV capacitor admittance. The resultant Fourier domain equivalent circuit is shown in Fig. 1(b) wherein the relevant node voltages and branch currents are labeled. By applying KCL at the node in the i^{th} branch, its voltage, $\underline{V_i}$, is given by:

$$\underline{V_i}(\omega) = \left(\mathbb{G}_i + \mathbb{G}_j + \mathbb{Y}_L\right)^{-1}\left(\mathbb{G}_i\underline{V_{o+}}(\omega) + \mathbb{G}_j\underline{V_{o-}}(\omega)\right), \quad (7)$$

where $j = \left(i + \frac{N}{2}\right) \bmod N$. Similarly, applying KCL at the positive terminal of the differential output, i.e. $\underline{V_{o+}}$, gives:

$$\underline{V_{o+}}(\omega) = \left(2\mathbb{G}_s + \sum_{i=0}^{N-1}\mathbb{G}_i\right)^{-1}\left[\mathbb{G}_s\underline{V_s}(\omega) + \sum_{i=0}^{\frac{N}{2}-1}\left(\mathbb{G}_i\underline{V_i}(\omega) + \mathbb{G}_j\underline{V_j}(\omega)\right)\right]. \quad (8)$$

The voltage at the negative terminal of the output, $\underline{V_{o-}}$, can be obtained in exactly the same manner. Hence, the total output differential voltage, $\underline{V_o} = \underline{V_{o+}} - \underline{V_{o-}}$, is given by:

$$\underline{V_{o+}}(\omega) - \underline{V_{o-}}(\omega) = \left(2\mathbb{G}_s + \sum_{i=0}^{N-1}\mathbb{G}_i\right)^{-1}\left[2\mathbb{G}_s\underline{V_s}(\omega) + \sum_{i=0}^{\frac{N}{2}-1}\left(\mathbb{G}_i - \mathbb{G}_j\right)\left(\underline{V_i}(\omega) - \underline{V_j}(\omega)\right)\right].$$

Substituting the value of $\underline{V_i}(\omega) - \underline{V_j}(\omega)$ (with expressions for $\underline{V_i}$ and $\underline{V_j}$ obtained using (7)), and simplifying, the final output is given by:

$$\underline{V_o}(\omega) = 2\left[2\mathbb{G}_s + \sum_{i=0}^{N-1}\mathbb{G}_i - \sum_{i=0}^{\frac{N}{2}-1}\left\{\left(\mathbb{G}_i - \mathbb{G}_j\right)\left(\mathbb{G}_i + \mathbb{G}_j + \mathbb{Y}_L\right)^{-1}\left(\mathbb{G}_i - \mathbb{G}_j\right)\right\}\right]^{-1}\mathbb{G}_s\underline{V_s}(\omega). \quad (9)$$

Thus, the LPTV transfer function, $\mathbb{H}(\omega)$, defined as $\underline{V_o}(\omega) = \mathbb{H}(\omega)\underline{V_s}(\omega)$ is obtained. The components of $\mathbb{H}(\omega)$ give the required HTFs $\{H_n(\omega)\}$ as shown in (3).

These expressions can be evaluated given numerical circuit components, as illustrated below for an example filter. Note that these expressions are completely general, and do not put any restrictions, such as ideal or non-overlapping clocks. Considering clock non-idealities is very easy in the proposed technique: only the LPTV conductance matrices, $\mathbb{G}_i$, needs to be altered according to the actual resistance variation. To illustrate, consider the case of duty-cycle variation in the clocks. In the ideal case, all the clocks have a duty cycle of $\frac{1}{N}$, but suppose the actual duty cycle of the clocks is $\frac{1}{N}(1-\beta)$ ($\beta = 0$ being the ideal case). Note that a negative β implies that the clocks are overlapping. Assuming an OFF conductance, G_{off}, and an ON conductance, G_{on}, $\mathbb{G}_i$ can be found from the corresponding periodic conductance variation, $G_i(t)$ (shown in Fig. 1(b)). The coefficient of $e^{jm\omega_p t}$ in the Fourier series of $G_i(t)$ is:

$$G_{i,m} = \frac{1}{m\pi}\left(G_{on} - G_{off}\right)sin\left(\frac{(1-\beta)m\pi}{N}\right)exp\left(-j\frac{2\pi im}{N}\right), \quad (10)$$

with $G_{i,0} = \frac{1-\beta}{N}(G_{on} - G_{off}) + G_{off}$.

In the following, let $G_{on}/G_{off} = 10^5$, and switching frequency $\omega_p = 2\pi/T_p$ be such that $\omega_p/\omega_{RC} = 31.4$ (similar to [11] for direct comparison), where $\omega_{RC} = 2/NR_sC$. A value of $K = 2000$ was used in (3) for constructing all conversion matrices. All simulation results are from Cadence SPECTRE PSS-PAC simulations, where the switches were modeled as periodically varying conductors using Verilog-A (unless specified).

A. Frequency Response

The HTFs, $\{H_n(\omega)\}$, give the frequency response of the circuit, and can be easily obtained from the entries of $\mathbb{H}(\omega)$. Thus, the magnitudes of the HTFs of a differential 4-path filter with ideal clock edges and extremely small switch resistance ($G_{on}R_s/2 = 10^3$) were calculated, and are shown in Fig. 2. These compare very well with results from prior art [11].

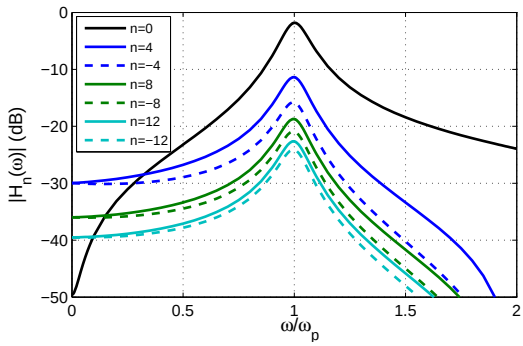

Figure 2. Magnitude of HTFs $\{H_n(\omega)\}$ for a 4-path filter around the switching frequency

These responses (except $H_o(\omega)$) can be regarded as folding responses of the filter, while $H_0(\omega)$ represents the filter response. This occurs as the output is essentially "sampled" with a sampling period of T_p/N. Hence, inputs at frequencies $kN\omega_p + \omega$ (k is an integer) fold on top of each other due to aliasing. Thus to reduce this folding, N has to be increased (ideally to infinity). However, this comes at the cost of reduced filtering of the harmonics, i.e. harmonic rejection, in $H_0(\omega)$. To confirm, the calculated magnitude of $H_0(\omega)$ is plotted in Fig. 3 for $N = 4$ and 8. The values are again in excellent agreement with prior art [11].

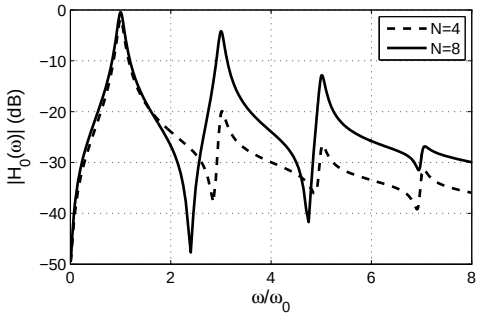

Figure 3. Magnitude of $H_0(\omega)$ for $N = 8$ vs. $N = 4$

B. Impact of Non-idealities

1) Switch ON Resistance: It is well known that the switch ON resistance, $1/G_{on}$, limits filter attenuation [11]. This can be simply understood as follows: far from the filter center frequency, the capacitors have zero impedance. Hence the maximum attenuation is approximately $-20\log_{10}[(1/G_{on})/(1/G_{on} + R_s/2)] = 20\log_{10}[1 + G_{on}R_s/2]$. The calculated filter response, $H_0(\omega)$, plotted in Fig. 4 agrees with this intuition, and matches with simulation results.

2) Non-ideal Duty Cycle Clocks: The effect of non-ideal duty cycle clocks (which may even introduce clock overlaps) on $H_0(\omega)$ can be easily studied by using non-zero values of β. Fig. 5 shows the calculated $H_0(\omega)$ for two values of β, alongside simulation results from verifying them. For $\beta = 0.2$, i.e. the case where all the switches are OFF for a certain period of time, the filtering response still retains a few peaks, but filter

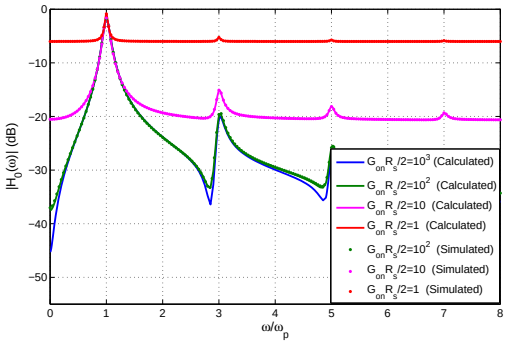

Figure 4. Magnitude of $H_0(\omega)$ for varying switch G_{on}

attenuation reduces to about 15dB. In the case of $\beta = -0.2$, i.e. overlapping clocks, the filtering response has completely degraded. This is a well known empirical result and occurs due to charge sharing between the load capacitors, but was not predicted by prior art.

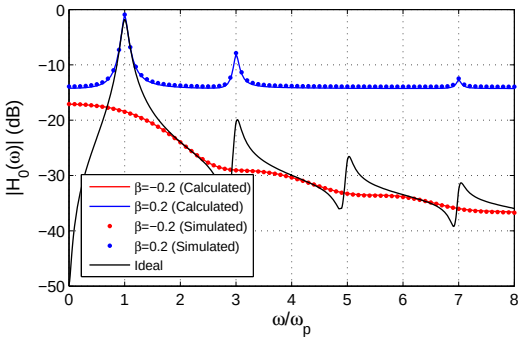

Figure 5. Magnitude of $H_0(\omega)$ for a 4-path filter in the case of imperfect duty-cycle clocks

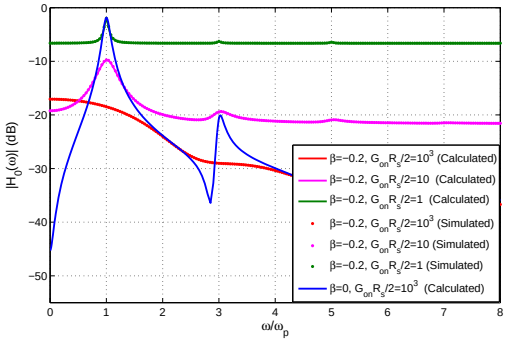

Figure 6. Magnitude of $H_0(\omega)$ with overlapping clocks and varying switch G_{on}

It's also interesting to see how the extent of degradation in $H_0(\omega)$ in case of overlapping clocks actually depends on the switch ON resistance. Fig. 6 shows the calculated and simulated $H_0(\omega)$ for various values of switch ON conductance, G_{on}. It can be readily noted that the degradation is worse for higher values of G_{on}. This is intuitive as higher switch ON resistance reduces the extent of charge sharing between load capacitors. Of course, this comes at the expense of lower filter attenuation due to lower G_{on} as seen in Fig. 4. Again,

this was not predicted in prior art, and was only known from simulations [11].

3) Switch Parasitic Capacitance: We can also consider parasitic elements. For example, if the switches introduce parasitic capacitors C_p at nodes V_{o+} and V_{o-} in the circuit, the final output can be easily shown to be:

$$\underline{V_o}(\omega) = 2\Bigg[2\mathbb{G}_s + \mathbb{Y}_p + \sum_{i=0}^{N-1}\mathbb{G}_i - \sum_{i=0}^{\frac{N}{2}-1}\Big\{(\mathbb{G}_i - \mathbb{G}_j)\left(\mathbb{G}_i + \mathbb{G}_j + \mathbb{Y}_L\right)^{-1}(\mathbb{G}_i - \mathbb{G}_j)\Big\}\Bigg]^{-1}\mathbb{G}_s\underline{V_s}(\omega), \tag{11}$$

where $\mathbb{Y}_p = jC_p\mathbf{\Omega}(\omega)$. Note that (11) is exactly the same as (9) with the exception of the presence of $\mathbb{Y}_p$. If we denote $C_p = \alpha C$, then the calculated and simulated filter responses are shown in Fig. 7. Notice that the filter gain and center frequency has degraded when C_p is just 10% of the load capacitance, C. This is an important result that is yet to be mentioned in prior art (and in fact limits the sizes of switches that can be used, and hence G_{on}).

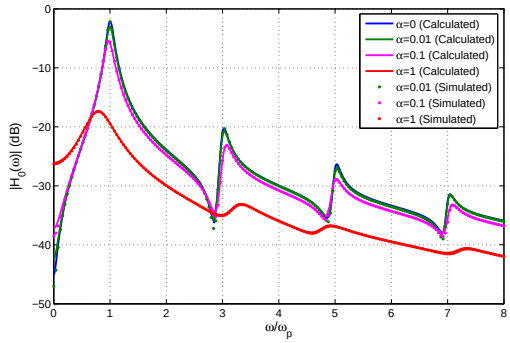

Figure 7. Magnitude of $H_0(\omega)$ with parasitic capacitors

C. Real Switches

Finally, the switches were also implemented (in schematic) using TSMC 65-nm CMOS process as transmission gates consisting of a pMOS and an nMOS transistor with $w/L = 0.5\mu m/60nm$, and M fingers each, biased at $V_{dd}/2$, and driving $C = 50pF$. They are driven by non-overlapping clocks operating at $500MHz$ with linear rising/falling edges lasting $50ps$ each and swinging from 0 to $V_{dd} = 1.2V$. For calculations, the switch parasitics and conductance variations were obtained from simulations (their Fourier coefficients were calculated using FFTs). The simulated and calculated results for various values of M are shown in Fig. 8, and clearly show the trade-off between filter attenuation and gain at center frequency due to G_{on} and C_p, respectively.

IV. Conclusions

In this paper, an analysis of N-path filters using conversion matrices is presented. The approach uses conversion matrices that allows LPTV circuits to be analyzed using familiar circuit theorems such as Kirchhoff's laws, in a manner similar to LTI circuits. Important results found in prior art were reproduced to verify the analysis technique and the effects of a few, but important circuit non-idealities not considered in prior art were also calculated.

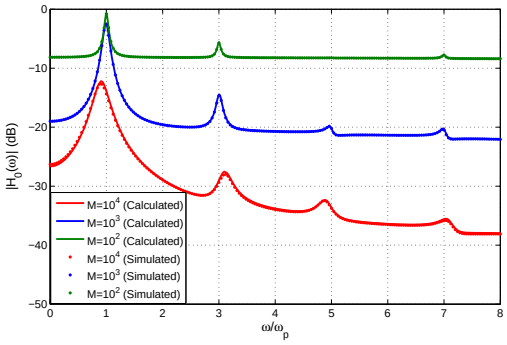

Figure 8. Magnitude of $H_0(\omega)$ for real switches

References

[1] Nekovee, M., "Cognitive Radio Access to TV White Spaces: Spectrum Opportunities, Commercial Applications and Remaining Technology Challenges," *New Frontiers in Dynamic Spectrum, 2010 IEEE Symposium on* , vol., no., pp.1,10, 6-9 April 2010.

[2] Abidi, A.A., "The Path to the Software-Defined Radio Receiver," *Solid-State Circuits, IEEE Journal of* , vol.42, no.5, pp.954,966, May 2007.

[3] L. E. Franks and I. W. Sandberg, "An alternative approach to the realization of network transfer functions: The N-path filters," *Bell Sys. Tech. J.*, vol. 39, pp. 1321–1350, Sep. 1960.

[4] Zadeh, Lotfi A, "Frequency Analysis of Variable Networks," *Proceedings of the IRE* , vol.38, no.3, pp.291,299, March 1950.

[5] El Oualkadi, A.; El Kaamouchi, M.; Paillot, J.-M.; Vanhoenacker-Janvier, D.; Flandre, D., "Fully Integrated High-Q Switched Capacitor Bandpass Filter with Center Frequency and Bandwidth Tuning," *Radio Frequency Integrated Circuits (RFIC) Symposium, 2007 IEEE* , vol., no., pp.681,684, 3-5 June 2007.

[6] Mirzaei, A.; Darabi, H.; Leete, J.C.; Yuyu Chang, "Analysis and Optimization of Direct-Conversion Receivers With 25% Duty-Cycle Current-Driven Passive Mixers," *Circuits and Systems I: Regular Papers, IEEE Transactions on* , vol.57, no.9, pp.2353,2366, Sept. 2010.

[7] Mirzaei, A.; Darabi, H., "Analysis of Imperfections on Performance of 4-Phase Passive-Mixer-Based High-Q Bandpass Filters in SAW-Less Receivers," *Circuits and Systems I: Regular Papers, IEEE Transactions on* , vol.58, no.5, pp.879,892, May 2011.

[8] Yuh Sun; Frisch, I.T., "A General Theory of Commutated Networks," *Circuit Theory, IEEE Transactions on* , vol.16, no.4, pp.502,508, Nov 1969.

[9] Strom, T.; Signell, S., "Analysis of periodically switched linear circuits," *Circuits and Systems, IEEE Transactions on* , vol.24, no.10, pp.531,541, Oct 1977.

[10] Soer, M. C M; Klumperink, E.A.M.; de Boer, P.-T.; van Vliet, F.E.; Nauta, B., "Unified Frequency-Domain Analysis of Switched-Series- RC Passive Mixers and Samplers," *Circuits and Systems I: Regular Papers, IEEE Transactions on* , vol.57, no.10, pp.2618,2631, Oct. 2010.

[11] Ghaffari, A.; Klumperink, E.A.M.; Soer, M. C M; Nauta, B., "Tunable High-Q N-Path Band-Pass Filters: Modeling and Verification," *Solid-State Circuits, IEEE Journal of* , vol.46, no.5, pp.998,1010, May 2011.

[12] Vanassche, P.; Gielen, G.; Sansen, Willy, "Symbolic modeling of periodically time-varying systems using harmonic transfer matrices," *Computer-Aided Design of Integrated Circuits and Systems, IEEE Transactions on* , vol.21, no.9, pp.1011,1024, Sep 2002.

[13] S. A. Maas, *Nonlinear microwave and RF circuits*, 2nd Ed., Artech House, 2003.

[14] Chua, L.O.; Ng, C.Y., "Frequency-domain analysis of nonlinear systems: formulation of transfer functions," *Electronic Circuits and Systems, IEE Journal on* , vol.3, no.6, pp.257,269, November 1979.

[15] Kundert, K.S.; Sangiovanni-Vincentelli, A, "Simulation of Nonlinear Circuits in the Frequency Domain," *Computer-Aided Design of Integrated Circuits and Systems, IEEE Transactions on* , vol.5, no.4, pp.521,535, October 1986.

[16] Roychowdhury, J.; Long, D.; Feldmann, P., "Cyclostationary noise analysis of large RF circuits with multi-tone excitations," *Custom Integrated Circuits Conference, 1997., Proceedings of the IEEE 1997* , vol., no., pp.383,386, 5-8 May 1997.